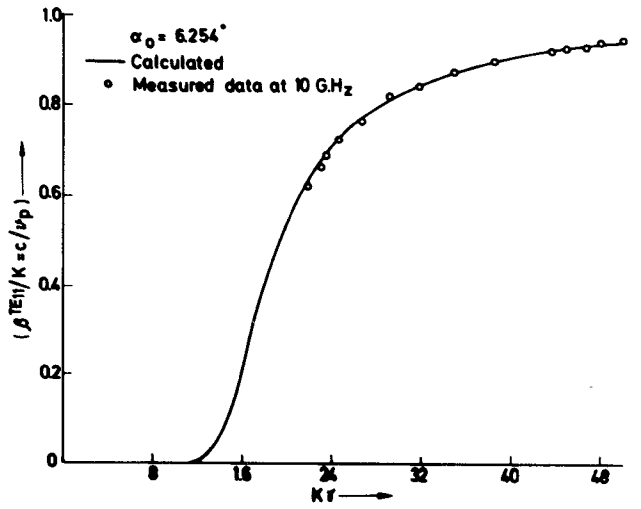

Fig. 7. Comparison of calculated and measured values for β/k for the TE_{11} mode.

has also been presented in the same figure for several values of α_0.[3] It has also been assumed here that the TE_{11} and TM_{11} modes are in phase at a radial distance $\alpha_1 = y$, where y is the eigenvalue for the TM_{11} mode for a prescribed α_0, since given a spherical mode, a cutoff radius may be approximately defined by $kr_c \doteq y$.

Finally, in order to examine the validity of the analytical procedure employed to study the transmission characteristics of spherical TE and TM modes in conical waveguides, measured data on (β/k) for a cone with $\alpha_0 = 6.254°$ at 10 GHz has been compared with the computed results in Fig. 7 for the TE_{11} mode. Excellent agreement between the two justifies the validity of the analysis presented.

IV. CONCLUSIONS

In conclusion one observes that a detailed study of the transmission characteristics of spherical TE and TM modes in conical waveguides is facilitated by accurate computation of eigenvalues. Further, the digital-computer based iterative procedure proposed for the evaluation of accurate eigenvalues of the spherical waves has been found to be very fast and highly accurate. Study of transmission characteristics of the spherical TE and TM modes within the guide has revealed a number of interesting properties. Explicit expressions are derived for various transmission parameters (attenuation constant, phase constant, and the wave impedance) associated with the mode transmission in a conical waveguide. These parameters are dependent on α_0 as well as the radial distance kr. A particular mode transmitted in a conical waveguide has to pass through an attenuation and a transmission region. The former is confined to the vicinity of the apex where the induction field predominates. At distances far away $(kr \geq y)$ from the apex there is a region of unattenuated transmission. A study of the phase slip between the spherical TE_{11} and TM_{11} modes transmitted simultaneously in a dual-mode conical waveguide has also been made. Experimental verification of the computed results on phase velocity of the spherical modes in conical waveguides justifies the validity of the analysis presented.

ACKNOWLEDGMENT

The authors wish to thank Dr. A. C. Ludwig, Jet Propulsion Laboratory, California Institute of Technology, California, for having supplied measured data on the phase velocity in a conical waveguide. They also wish to thank the Computer Center, IIT-Madras for having provided the facilities of IBM-370/155 System for the numerical computations involved in this short paper.

[3] It may be pointed out that the lower limit of the integral (2) is taken to be $\alpha_1 = y$ (where "y" is the eigenvalue for the TM_{11} mode) since one is primarily interested in the relative phase shift between the dominant spherical TE and TM modes in a dual mode conical waveguide. Further, in a dual-mode concial waveguide, the TM_{11} mode is generated by introducing a discontinuity at a radial distance $kr_1 = y$. Hence it follows that $\alpha_1 = kr_1 = y$.

REFERENCES

[1] E. C. Okress, *Microwave Power Engineering*, vol. 1. New York: Academic, 1968, pp. 228–240.
[2] P. D. Potter, "A new horn antenna with suppressed side lobes and equal beamwidth," *Microwave J.*, vol. 6 pp. 71–78, June 1963.
[3] R. F. Harrington, *Time-Harmonic Electromagnetic Fields*. New York: McGraw-Hill, 1961, ch. 6.
[4] M. S. Narasimhan and B. V. Rao, "Hybrid modes in corrugated conical horns," *Electron. Lett.*, vol. 6, pp. 32–34, Jan. 1970.
[5] M. A. Abramovitz and A. I. Stegun, *Hand Book of Mathematical Functions*. New York: Dover, 1965, ch. 9.
[6] W. Magnus and F. Oberhettinger, *Formulas and Theorems for the Functions of Mathematical Physics*. New York: Chelsea, 1954, pp. 72 and 67.
[7] J. M. McCormick and M. G. Salvadori, *Numerical Methods in Fortran*. Englewood Cliffs: N. J.: Prentice-Hall, 1964, ch. 4.

Simple Stabilizing Method for Solid-State Microwave Oscillators

A. KONDO, T. ISHII, AND K. SHIRAHATA

***Abstract*—In the microwave solid-state oscillators using bulk effect and avalanche diodes, high dielectric constant ceramics have been used as a temperature compensator and excellent temperature stability is obtained. An X-band avalanche diode oscillator is tested over a wide temperature range. The frequency drift is improved to be less than +30 kHz/°C. Additional advantages of this technique are compact size and low cost.**

I. INTRODUCTION

A simple means of reducing the noise and stabilizing the solid-state microwave oscillator is to use a high-Q cavity stabilizer. A phase lock technique has also been used by means of an injected signal and a mechanical compensation method which uses a tuning rod having a large temperature coefficient of expansion in the cavity. But these methods are fairly troublesome.

In this short paper, simple stabilizing methods using a ceramic dielectric are described. A ceramic dielectric which has a negative temperature coefficient is loaded in parallel with the diode package. The change of the diode and circuit reactance with temperature can be compensated by the capacitance change of the dielectric. A temperature coefficient less than +30 kHz/°C is obtained in a low-Q X-band cavity. These methods have merits of simplicity and low cost.

II. TEMPERATURE STABILIZATION WITH A DIELECTRIC

The effect of temperature on the diode reactance is due to the variation of the carrier velocity and the derivative of the ionization coefficient. These two parameters decrease with the temperature increase and it results in the increase of diode inductance. The increase of reactance causes the oscillation frequency to shift lower when the bias current is held constant. The cavity expansion due to the temperature rise also invites the same results on frequency characteristics.

If the change of diode and cavity reactance is trimmed with a ceramic capacitor having negative temperature coefficient, the oscillator would maintain the same frequency over the operating temperature range. Some titanium oxide dielectrics have negative temperature coefficients of capacitance [1]. Fortunately, its dielectric losses are the same order of alumina ceramics which are used for the microwave diode's package. In the following, we consider the circuit parameters to be represented by lumped constants. Judging from experimental results this assumption is reasonable at X band.

The oscillation frequency of an avalanche diode oscillator decreases almost rectilinearly with the temperature rise. We consider such an equivalent circuit as Fig. 1. C_p is the capacitance of the diode package and it changes very little with temperature. L_e is the equivalent inductance of the oscillator circuit. G and G_e represent

Manuscript received May 28, 1974.
The authors are with the Central Research Laboratory, Mitsubishi Electric Corporation, Itami, Hyogo, Japan.

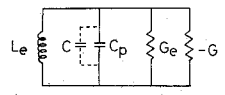

Fig. 1. Equivalent circuit of avalanche diode oscillator having temperature compensated diode.

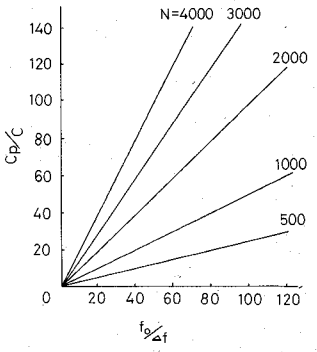

Fig. 2. Relation between C_p/C and $f_0/\Delta f$ as a function of temperature coefficient.

the diode negative conductance and circuit conductance. The oscillation frequency decreases with the temperature rise and its temperature coefficient is α_1. The oscillation frequency is written as

$$\omega_0(1 - \alpha_1 T) = \frac{1}{L_e C_p} \tag{1}$$

so that

$$L_e = \frac{1}{\omega_0^2 C_p}(1 + 2\alpha_1 T). \tag{2}$$

The equivalent inductance has a temperature coefficient of $2\alpha_1$. When the ceramic capacitor C having a negative temperature coefficient β_1 is parallel with the ceramic package, the resonant frequency is given as

$$\omega = \frac{\omega_0}{1 + C/C_p}\left\{1 - \frac{1}{2}\frac{(C/C_p)(2\alpha_1 - \beta_1) + 2\alpha_1}{1 + C/C_p} T\right\}. \tag{3}$$

Selecting $C_p/C \gg 1$, the condition of stabilization with temperature is

$$\beta_1 = 2\alpha_1 C_p/C. \tag{4}$$

Thus the temperature compensation of oscillation can be achieved and the oscillation frequency is written as

$$\omega = \omega_0(1 - C/2C_p). \tag{5}$$

Equation (4) is reduced as

$$CN = 2000(\Delta f/f_0)C_p \tag{6}$$

where f_0 is in gigahertz, the temperature coefficient of ceramic N is in parts per million per degree centigrade, the frequency deviation Δf is in megahertz per degree centigrade, and C, C_p are in picofarads, respectively. The relation between C_p/C and $f_0/\Delta f$ is shown in Fig. 2 with N as a parameter. It is necessary for temperature compensation to know the capacitance of the ceramic package C_p, the oscillation frequency f_0 at a standard temperature, and the frequency deviation Δf with temperature. The temperature coefficient of the ceramic condenser N and C_p/C are determined from $f_0/\Delta f$ in Fig. 2, and then the ceramic capacitance C is determined.

III. EXPERIMENTAL RESULTS

In the experiment of compensation with the parallel capacitor, the external Q of the oscillator cavity is about 20. A ceramic capacitor[1] is cut 100 × 300 μm wide and 800 μm in length and both ends are soldered to the metal electrode of the diode package. The photograph of these diodes is shown in Fig. 3. In the picture the dark line parts of diode packages are ceramic compensators.

The experimental results of power and frequency are shown in Fig. 4. When the diode has no ceramic compensator, the oscillation frequency is 9.845 GHz at 6°C and the temperature coefficient is −110 kHz/°C over the temperature range from 42° to +55°C. While the measured temperature coefficient of the oscillator using the ceramic compensator is less than +30 kHz/°C and the oscillation frequency is 9.408 GHz at 10°C. The frequency deviation is less than 2 MHz over the temperature range of about 60°C. The frequency meter used here is model 312 A of EIP Laboratories and the reading accuracy is in megahertz units. By changing the ceramic compensator to have narrower electrode spacing and a larger capacitance, the frequency characteristic shows over compensation. The temperature coefficient is +180 kHz/°C and the oscillation frequency is 9.224 GHz at 2°C

This result shows that we can change the temperature coefficient of oscillator frequency by selection of the capacitance of a ceramic capacitor and its temperature coefficient. The temperature coefficient of the ceramic compensator is −2200 ppm/°C in nominal value. Oscillator's $f/\Delta f$ of the noncompensated one is 86, C_p is 0.8 pF, and C is 0.01 pF at 1 MHz. From Fig. 2, N is about 1900. Judging from the nominal value of the ceramic capacitor's temperature coefficient, this result is fairly reasonable. From the second term in the parentheses of (3), the temperature coefficient is to be +20 kHz/°C. The difference from the experimental value of +30 kHz/°C is, first, because the equivalent circuit is not shown precisely as in Fig. 1, owing to parasitic elements of the diode and, second, because the package parameter does not act perfectly as the lumped constant at microwave frequency.

The advantage of this method is to compensate the frequency drift with temperature by attaching a tiny ceramic on the diode package. Capacitance of the ceramic compensator is in the deviation of the ceramic package's capacitance and there is little effect upon the output power.

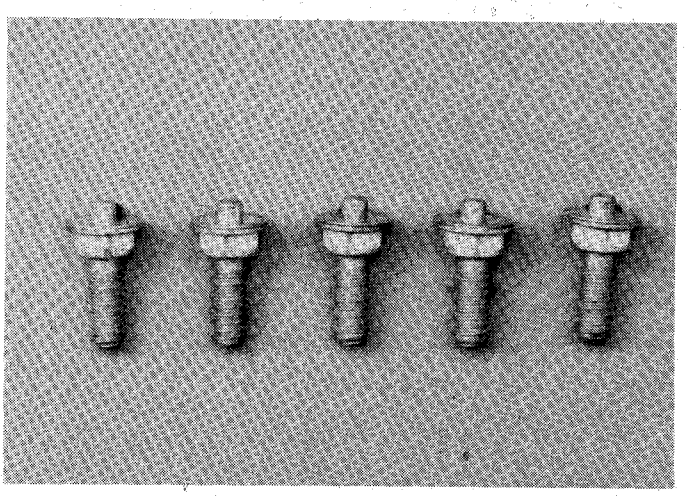

Fig. 3. Temperature compensated avalanche diode with parallel capacitor.

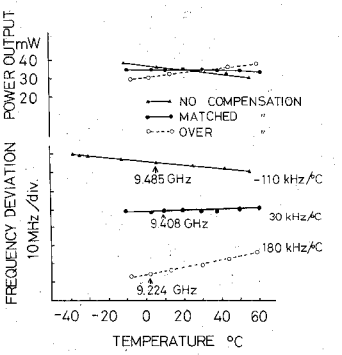

Fig. 4. Measured temperature characteristics of avalanche diode oscillator using temperature compensated diode.

[1] Commercial product's condenser of Tokyo Denki Kagaku for temperature compensation. Its nominal value of temperature coefficient is −2200 ppm/°C.

IV. CONCLUSION

The simple temperature compensated oscillator has been designed for use with avalanche transit time diodes. A ceramic capacitor which has a negative temperature coefficient is used for a temperature compensator. Stabilized oscillators are improved considerably in performance compared with nonstabilized oscillators of the same cavity.

The frequency drift in the low-Q cavity having parallel ceramic capacitor with the diode package is less than +30 kHz/°C. These compensation techniques need no additional structures such as a stabilized cavity and a mechanical compensating tuner. Especially, simplicity, low cost, and compact size are the main advantages of employing the ceramic loading on the diode package to compensate for temperature changes. Moreover, since this technique is completely passive, no power is required and the frequency stability shows the same results as the mechanical tuning compensation.

REFERENCES

[1] R. Von Hippel, *Dielectric Material and Applications*. New York: Technology Press of M.I.T. and Wiley, 1954.

Letters

Comments on "Rectangular Waveguides with Impedance Walls"

P. R. McISAAC

In the above paper,[1] Dybal *et al.* discuss the propagation characteristics of several rectangular waveguides with corrugated walls and analyze them by using impedance boundaries to simulate the corrugated walls. One of the waveguides discussed, called an E guide, has longitudinal corrugations in all four walls. The authors claim that this waveguide will support E modes but not H modes. However, this waveguide has an isotropic homogeneous dielectric surrounded by a conducting boundary which is longitudinally uniform. Therefore, if the boundary is assumed to be a perfect conductor, this waveguide must support a complete set of both E and H modes; the presence of the corrugations cannot change this conclusion.

In their discussion of the E guide in Section III,[1] the authors state that the wall impedances $Z_2 = Z_3 = 0$, $Z_1 \neq 0$, $Z_4 \neq 0$ (refer to their paper for the definitions of these impedances) may be used to simulate a rectangular waveguide with longitudinally corrugated walls. They assert as follows.

> "The ordinary E modes satisfy the impedance boundary conditions for this impedance configuration while the H modes do not."

They also assert the following.

> "Modal solutions other than E modes have field components that are incompatible with the impedance boundary conditions."

No proof is offered for these assertions.

In fact, these assertions are not correct. Consider the following set of electromagnetic field components in the region: $-W/2 < x < W/2$, $-H/2 < y < H/2$ (for convenience, the origin of the coordinate system is shifted to the center of the waveguide, see Fig. 1[1]). The notation is essentially that used in the original paper.[1]

$$E_x = \frac{-j\omega\mu}{\Gamma^2 + k^2} K_y H_0 \sin (K_x x) \cos (K_y y) \exp (-\Gamma z)$$

$$E_y = \frac{j\omega\mu}{\Gamma^2 + k^2} K_x H_0 \cos (K_x x) \sin (K_y y) \exp (-\Gamma z)$$

$$E_z = 0$$

$$H_x = \frac{-\Gamma}{\Gamma^2 + k^2} K_x H_0 \cos (K_x x) \sin (K_y y) \exp (-\Gamma z)$$

$$H_y = \frac{-\Gamma}{\Gamma^2 + k^2} K_y H_0 \sin (K_x x) \cos (K_y y) \exp (-\Gamma z)$$

$$H_z = H_0 \sin (K_x x) \sin (K_y y) \exp (-\Gamma z).$$

It is easily verified that these field components satisfy all of Maxwell's equations if

$$\Gamma^2 + k^2 - K_x^2 - K_y^2 = 0.$$

In addition, this set of field components is compatible with the impedance conditions at the walls stated by the authors. Assuming that the nonzero wall impedances are reactive, so that $Z_1 = jX_1$ and $Z_4 = jX_4$, the boundary conditions at the walls are

$$jX_1 = \frac{-E_x(x,H/2)}{H_z(x,H/2)}, \qquad \text{at } y = H/2$$

$$jX_4 = \frac{E_y(W/2,y)}{H_z(W)2,y)}, \qquad \text{at } x = W/2$$

with analogous expressions at the other walls.

Inserting the field components given above into these boundary conditions, one obtains

$$(K_y H/2) \cot (K_y H/2) = \frac{\Gamma^2 + k^2}{k^2} \frac{kH}{2} \frac{X_1}{Z_0}$$

$$(K_x W/2) \cot (K_x W/2) = \frac{\Gamma^2 + k^2}{k^2} \frac{kW}{2} \frac{X_4}{Z_0}.$$

This pair of equations, together with

$$\Gamma^2 + k^2 - K_x^2 - K_y^2 = 0$$

are sufficient to determine the k versus Γ relationship for given vaues of H, W, X_1, and X_4.

There are an infinite set of solutions to the pair of transcendental equations just given. In addition to these solutions, there are three other infinite sets of solutions that can be obtained, based on

$$H_z = H_0 \sin (K_x x) \cos (K_y y) \exp (-\Gamma z)$$

$$H_z = H_0 \cos (K_x x) \sin (K_y y) \exp (-\Gamma z)$$

$$H_z = H_0 \cos (K_x x) \cos (K_y y) \exp (-\Gamma z)$$

respectively. Therefore, contrary to the assertion made in the paper,[1] the impedance wall model used there has an infinite set of H modes.

Manuscript received November 16, 1973.

The author is with the Department of Electrical Engineering, Cornell University, Ithaca, N. Y. 14850.

[1] R. B. Dybal, L. Peters, Jr., and W. H. Peake, *IEEE Trans. Microwave Theory Tech.*, vol. MTT-19, pp. 2–9, Jan 1971.